MPMI Vol. 35, No. 9, 2022, pp. 857–866, https://doi.org/10.1094/MPMI-05-22-0108-R

# The XadA Trimeric Autotransporter Adhesins in *Xylella fastidiosa* Differentially Contribute to Cell Aggregation, Biofilm Formation, Insect Transmission and Virulence to Plants

**Oseias R. Feitosa-Junior,[1] Ana Paula S. Souza,[1] Paulo A. Zaini,[1,2] Clelia Baccari,[3] Michael Ionescu,[3] Paulo M. Pierry,[1] Guillermo Uceda-Campos,[1] Fabien Labroussaa,[4,5] Rodrigo P. P. Almeida,[4] Steven E. Lindow,[3,†] and Aline M. da Silva[1,†]**

[1] Departamento de Bioquímica, Instituto de Química, Universidade de São Paulo, São Paulo, Brazil
[2] Department of Plant Sciences, University of California, Davis, CA, U.S.A.
[3] Department of Plant and Microbial Biology, University of California, Berkeley, U.S.A.
[4] Department of Environmental Science, Policy and Management, University of California, Berkeley, U.S.A.
[5] Institute of Veterinary Bacteriology, Vetsuisse Faculty, University of Bern, Bern, Switzerland

Accepted for publication 13 June 2022.

**Surface adhesion strategies are widely employed by bacterial pathogens during establishment and systemic spread in their host. A variety of cell-surface appendages such as pili, fimbriae, and afimbrial adhesins are involved in these processes. The phytopathogen *Xylella fastidiosa* employs several of these structures for efficient colonization of its insect and plant hosts. Among the adhesins encoded in the *X. fastidiosa* genome, three afimbrial adhesins, XadA1, Hsf/XadA2, and XadA3, are predicted to be trimeric autotransporters with a C-terminal YadA-anchor membrane domain. We analyzed the individual contributions of XadA1, XadA2, and XadA3 to various cellular behaviors both in vitro and in vivo. Using isogenic *X. fastidiosa* mutants, we found that cell-cell aggregation and biofilm formation were severely impaired in the absence of XadA3. No significant reduction of cell-surface attachment was found with any mutant under flow conditions. Acquisition by insect vectors and transmission to grapevines were reduced in the XadA3 deletion mutant. While the XadA3 mutant was hypervirulent in grapevines, XadA1 or XadA2 deletion mutants conferred lower disease severity than the wild-type strain. This insight of the importance of these adhesive proteins and their individual contributions to different aspects of *X. fastidiosa* biology should guide new approaches to reduce pathogen transmission and disease development.**

*Keywords*: afimbrial adhesin, biofilm, phytopathogen, Pierce's disease, YadA-anchor domain

[†]Corresponding authors: S. E. Lindow; icelab@berkeley.edu, and A. M. da Silva; almsilva@iq.usp.br

O. R. Feitosa-Junior and A. P. S. Souza contributed equally.

Current address for Michael Ionescu: Lavie Bio, Rehovot, Israel.

**Funding:** Funding for this work was provided by São Paulo Research Foundation (FAPESP) research grant 08/11703-4, by National Council for Scientific and Technological Development research grant 309182/2016-6, and by the Pierce's Disease Control Program of the California Department of Food and Agriculture. A. P. S. Souza, G. Uceda-Campos, P. A. Zaini, and P. M. Pierry were supported by FAPESP fellowships 14/03617-1, 21/04062-7, 11/09409-3, and 11/24091-0, respectively. O. R. Feitosa-Junior and G. Uceda-Campos received fellowships from the Coordination for the Improvement of Higher Education Personnel (CAPES). M. Ionescu was supported by the United States–Israel Binational Agricultural Research and Development Fund (BARD) Vaadia-BARD Postdoctoral Fellowship Award FI-427-09. A. M. da Silva received a Research Fellowship Abroad from FAPESP (award 10/16409-7).

***e*-Xtra:** Supplementary material is available online.

The author(s) declare no conflict of interest.



*Xylella fastidiosa* is the causal agent of several important diseases such as Pierce's disease of grapevine (PD), citrus variegated chlorosis, and olive quick decline syndrome in the United States, Brazil, and Italy (Sicard et al. 2018). This bacterium colonizes the xylem vessels of plants and the cuticular lining of the foregut of xylem–sap feeding insects that serve as obligate vectors, eventually forming persistent biofilm structures on these surfaces (Chatterjee et al. 2008; Rapicavoli et al. 2018). The biofilm structures are important for efficient retention and transmission by insect vectors and are crucial for successful *X. fastidiosa* plant colonization and virulence (Chatterjee et al. 2008; Killiny and Almeida 2014; Roper et al. 2019). Nevertheless, systemic spread through the xylem vessel network, which is associated with symptom progression in grapevines, requires dispersal of *X. fastidiosa* cells from biofilms as well as active motility via twitching and degradation of pit membranes by bacterial exoenzymes (Guilhabert and Kirkpatrick 2005; Meng et al. 2005; Nascimento et al. 2016; Newman et al. 2004; Roper et al. 2007). Accordingly, some *X. fastidiosa* mutants, such as *rpfF* (Newman et al. 2004), *hxfA* and *hxfB* (Guilhabert and Kirkpatrick 2005), and *prtA* (Gouran et al. 2016), defective in cell-cell aggregation, surface attachment, or biofilm maturation, display enhanced systemic colonization and a hypervirulent phenotype in susceptible plant hosts. In contrast, *X. fastidiosa* mutants compromised in exopolysaccharides (EPS) production and in biofilm formation present reduced virulence in grapevines. These EPS mutants present very low cell populations within

plants and reduced colonization compared with the wild-type strain (Killiny et al. 2013).

Bacterial cell-cell aggregation and attachment to plant tissues are mediated by cell surface–associated molecules, such as adhesins and exopolysaccharides (Danhorn and Fuqua 2007; Mhedbi-Hajri et al. 2011; Zaini et al. 2016). *X. fastidiosa* possesses several types of adhesins, including fimbrial adhesins of the short (type I) and long (type IV) pili (Li et al. 2007) and afimbrial adhesins, among them, the hemagglutinin-like proteins HxfA and HxfB (Guilhabert and Kirkpatrick 2005; Voegel et al. 2010), the autotransporter adhesin XatA (Matsumoto et al. 2012), and the *Xanthomonas* adhesin A-like orthologs XadA1 and XadA2 (previously called Hsf) (Caserta et al. 2010; Feil et al. 2007). *X. fastidiosa* mutants defective in the type-IV pilus adhesin are deficient in attachment to surfaces and thereby show reduced twitching motility (Li et al. 2007). On the other hand, mutants defective in the adhesin of type I pili do not aggregate on glass surfaces (Feil et al. 2007). HxfA and HxfB mediate cell-cell aggregation (Guilhabert and Kirkpatrick 2005) as well as adhesion to insect foregut surfaces (Killiny and Almeida 2009b).

The XadA proteins are predicted to belong to the family of trimeric autotransporter adhesins (TAA) (Caserta et al. 2010; Mhedbi-Hajri et al. 2011). TAAs within gram-negative bacteria comprise a family of cell-surface proteins that form homotrimers presenting a similar head-stalk-anchor architecture. The prototypical TAA is *Yersinia* adhesin A (YadA), in both *Yersinia enterocolitica* and *Yersinia pseudotuberculosis*, which mediates adhesion to the extracellular matrix components of eukaryotic host cells and is essential for the resistance of these pathogens to serum-induced bacterial lysis (Mühlenkamp et al. 2015). A common feature of the TAA monomers is a C-terminal YadA-anchor domain that trimerizes, thus producing a β-barrel structure serving as a transmembrane channel through which the passenger domain is externalized. The passenger domain typically folds as a coiled-coil stalk that projects the globular head away from the bacterial outer membrane (Fan et al. 2016; Hartmann et al. 2012; Meuskens et al. 2019).

While XadA1 is detected throughout the process of in vitro biofilm development in *X. fastidiosa* citrus variegated chlorosis strain 9a5c, XadA2 is detected primarily at later stages of biofilm formation (Caserta et al. 2010). A XadA1 mutant exhibited reduced initial attachment to glass surfaces, compared with the wild-type strain, and was less virulent to grapevines (Feil et al. 2007). XadA2 has been shown to be involved in *X. fastidiosa* adhesion to and transmission by vectors; while XadA2 has an affinity for plant and insect polysaccharides, it was not demonstrated to influence cell aggregation in vitro (Esteves et al. 2020). Transcription of *xadA1* and *xadA2* is upregulated in early stages of biofilm formation (de Souza et al. 2005) as well as in bacteria recovered from symptomatic periwinkle plants (de Souza et al. 2003). XadA1 is enriched in outer membrane vesicles (OMVs) produced by strain Temecula1 pathogenic to grapevine (Feitosa-Junior et al. 2019; Ionescu et al. 2014; Nascimento et al. 2016), apparently contributing to adherence of OMVs to surfaces. The *X. fastidiosa* genome encodes a third TAA protein, XadA3, which is strongly bound to the cell membrane (Smolka et al. 2003) and also detected in OMV-enriched fractions obtained from both strains 9a5c and Temecula1 (Feitosa-Junior et al. 2019).

Despite efforts to better understand the roles of various adhesins in *X. fastidiosa*, there are limited insights as to the relative individual contributions of XadA1, XadA2, and XadA3 to cell-cell aggregation, biofilm formation, cell-surface interactions, insect transmission, and virulence to plants. As these three XadA proteins belong to the TAA family, we hypothesized they would contribute equally to these various phenotypes, regardless of being differentially expressed during biofilm formation or being found to be associated to OMVs. To address this question, we investigated these phenotypes in single knockout mutants of strain Temecula1. We find that the *X. fastidiosa* TAAs contribute more to cell-cell aggregation and biofilm formation than to surface attachment when assayed under flow conditions mimicking their habitat in plants and insects. We also show that, while deletion of *xadA1* or *xadA2* attenuates *X. fastidiosa* virulence in grapevine, *xadA3* deletion elicits a hypervirulent phenotype and significantly reduces insect transmission.

## RESULTS

### XadA1, XadA2, and XadA3 are TAAs.

A typical C-terminal YadA-like anchor membrane domain (Pfam PF03895) was identified in XadA1 (PD0731) and XadA2 (PD0744) as well as in XadA3 (PD0824) protein sequences of *X. fastidiosa* Temecula1, with Pfam E values of $8 \times 10^{-8}$, $4 \times 10^{-16}$, and $4 \times 10^{-18}$, respectively. TAA head and stalk Pfam domains, termed YadA-head (PF05658) and YadA-stalk (PF05662), respectively, were also identified in all three XadA proteins (Fig. 1A), even if their relative positions and numbers vary among them. The monomers of the three Temecula1 TAAs were computationally modeled using Phyre2 software (Kelley et al. 2015), which uses homology detection methods to predict the three-dimensional structure. The predicted models for the three XadA proteins (Fig. 1B) reveal the YadA-anchor transmembrane domain and a coiled stalk typical of TAA family members, with confidence >90% and coverage of 80, 22, and 40% of the protein sequence of XadA1, XadA2, and XadA3, respectively. Altogether, analyses of the domain architecture of XadA1, XadA2, and XadA3 as well as predictions of their tridimensional structure strongly support conjectures that these proteins are TAA family members.

The sequence lengths predicted for the three Temecula1 TAA proteins differ substantially (997, 2,504, and 1,315 amino acids (aa) for XadA1, XadA2, and XadA3, respectively). The size discrepancies are mostly due to differences in the length of the segment encompassing the YadA-stalk and YadA-head domains (Fig. 1A). Phylogenetic analysis of the YadA-anchor domain reveals that the XadA2 and XadA3 YadA-anchor domain sequences group in a separate branch from XadA1 and distinct from the prototypical YadA-anchor domain from *Y. enterocolitica* and *Y. pseudotuberculosis* (Fig. 1C). It is noteworthy that orthologs of the three Temecula1 XadAs were found in the vast majority of complete or high-quality draft genomes of *X. fastidiosa* publicly available (Uceda-Campos et al. 2022). Despite variations in their sequence lengths among the many sequenced *X. fastidiosa* strains (815 to 1,004 aa for XadA1, 1,389 to 3,396 aa for XadA2, 940 to 1,440 aa for XadA3), the orthologs of each XadA are relatively highly conserved and have overall amino acid sequence similarities higher than 70% (not shown).

While a typical signal peptide was not clearly identified in the N terminal of either XadA1 or XadA3 (SignalP likelihood = 0.1905 and 0.0088, respectively), such a sequence was predicted with high confidence in XadA2 (SignalP likelihood = 0.8679). Notwithstanding, all three XadA proteins were predicted to be secreted by nonclassical pathways (SecP score = 0.93 to 0.96). In silico analysis using the pSortB tool suggested that the subcellular localization of XadA1 was both extracellular and in the outer membrane, while XadA2 and XadA3 were predicted to be located exclusively in the outer membrane. The outer membrane as the subcellular location for the various XadAs is supported by experimental evidence that shows that XadA1, XadA2, and XadA3 are, respectively, enriched in the outer membrane protein fraction (Ionescu et al. 2014; Nascimento et al. 2016), in the cell surface (Caserta et al. 2010), and strongly bound to the cell membrane (Smolka et al. 2003).

**XadA mutants differ in cell-cell aggregation, biofilm formation and motility phenotypes.**

The functional properties of the three XadA proteins were evaluated by assessing various phenotypes exhibited by Δ*xadA1*, Δ*xadA2*, and Δ*xadA3* deletion mutants compared with the parental wild-type strain (WT). To quantify cell-cell aggregation, equivalent concentrations of culture suspensions were monitored for precipitation of cell aggregates (autoaggregation) as a function of incubation time. Cells of the Δ*xadA3* mutant were found to sediment much more slowly than that of WT cells, indicative of reduced cell-cell aggregation (Fig. 2A and B). In contrast, cells of the Δ*xadA1* and Δ*xadA2* mutants clumped together and sedimented slightly faster than the WT strain, suggesting enhanced autoaggregation properties (Fig. 2B).

All three XadA mutants, most notably Δ*xadA2* and Δ*xadA3*, exhibited less biofilm formation on both glass and plastic surfaces after growth in periwinkle wilt medium (Davis et al. 1981) containing 0.5% glucose without bovine serum albumin (PWG) for 14 days (Fig. 2C and D). Unlike WT, none of the three mutant strains formed a robust biofilm on the sides of broth culture flasks within 7 days of growth (Supplementary Fig. S1). While each of the three Δ*xadA* mutants eventually formed at least a small biofilm at the liquid-air interface after longer incubation times (>14 days), these biofilms were less abundant than that of the WT strain and a much larger fraction of the Δ*xadA* mutant cells remained planktonic in the cultures (Supplementary Fig. S1).

We assayed surface adhesion using microfluidic chambers that mimic the flow conditions from xylem vessels (about 5 mm/s) and insect mouthparts (about 500 mm/s). Tracking of individual cells under increasing flow speeds revealed that the three *xadA* deletion mutants retained their ability to bind and resist detachment due to liquid flow forces similarly to WT. Only small reductions in the proportion of cells that adhered at the highest flow rates were observed, particularly for Δ*xadA*2 (Supplementary Fig. S2A). The lack of contribution of XadA3 to surface attachment was further confirmed in studies in which we incubated the WT strain with anti-XadA3 serum. No difference in the attachment of cells exposed to pre-immune serum and anti-XadA3 antibodies was observed (Supplementary Fig. S2B), indicating that blocking XadA3 does not alter cell-to-surface adhesion significantly.

Twitching motility can be detected as peripheral fringes that form around colonies on agar plates. All three Δ*xadA* mutants as well as the WT strain exhibited twitching motility activity and it was found to be more pronounced in colonies on PIM6 medium (Fig. 3) than on PWG (not shown). It is noteworthy that both Δ*xadA2* and Δ*xadA3* formed much wider colony fringes on PIM6 medium than did either the WT or the Δ*xadA1* mutant, suggesting that their active movement across the agar surface was less hindered by adhesion.

**XadA3 deletion impairs insect transmission and elicits hypervirulent phenotype in grapevine.**

The role of the XadA proteins in the combined processes of insect bacterial acquisition and efficiency of transmission to plants was assessed using an artificial diet system under controlled conditions in vitro (Killiny and Almeida 2009a). Transmission of mutants Δ*xadA1* and Δ*xadA2* were reduced on average by 32 and 43%, respectively, when compared with the WT strain (Fig. 4A). Remarkably, insect transmission of the Δ*xadA3* mutant was nearly completely abolished (Fig. 4A).

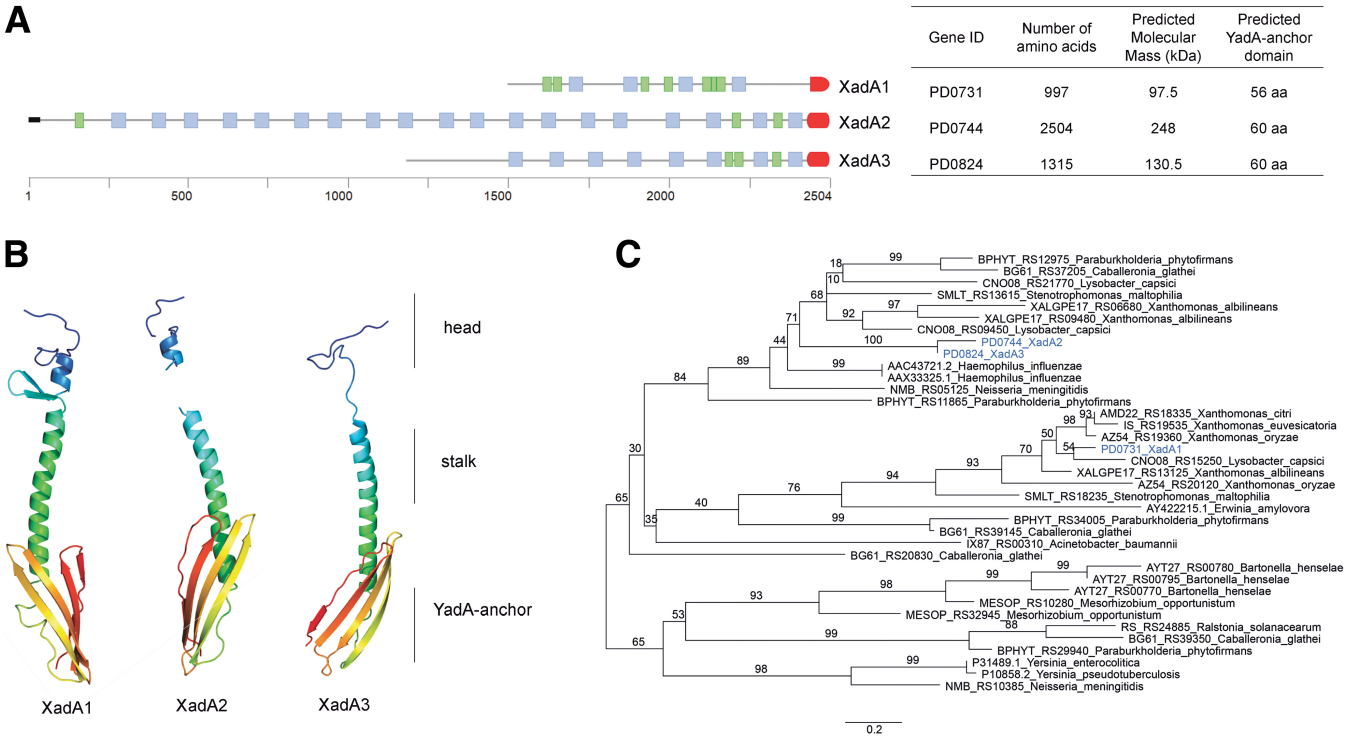


| Gene ID | Number of amino acids | Predicted Molecular Mass (kDa) | Predicted YadA-anchor domain |
|---|---|---|---|
| PD0731 | 997 | 97.5 | 56 aa |
| PD0744 | 2504 | 248 | 60 aa |
| PD0824 | 1315 | 130.5 | 60 aa |

**Fig. 1.** Trimeric autotransporter adhesins (TAA) of *Xylella fastidiosa*. **A,** Pfam domains identified in XadA1, XadA2, and XadA3 from the Temecula1 strain. The C-terminal YadA-anchor membrane domain is indicated in red. The blue and green blocks indicate YadA-head and YadA-stalk Pfam domains, respectively. An amino acid scale is shown below the XadA domain architecture schemes. The black block in XadA2 indicates signal peptide. The gene IDs for each XadA are from the Temecula1 original genome annotation. **B,** Structure prediction of TAA monomers modelled by Phyre2 software. Images are rainbow-colored from N (blue) to C (red) terminus. Regions of YadA-anchor, YadA-stalk, and YadA-head are noted. **C,** The maximum likelihood phylogenetic tree built from alignment of the YadA-anchor domain sequences of XadA1, XadA2, and XadA3 (written in blue) and YadA-anchor domains from proteins of the indicated bacterial species. Bootstrap confidence values at the branches were based on 1,000 replications. A branch length of 0.2 substitution per site is given to phylogenetic distances.

In addition to their interaction with the insect vectors, disease development in the plant host was also monitored after inoculation with the Δ*xadA* mutants. The contribution of XadAs to *X. fastidiosa* virulence was evaluated by comparison of the severity of PD symptoms as a function of time after inoculation with WT or each of the three *xadA* deletion mutants into the base of susceptible grapevines. Plants inoculated with Δ*xadA1* and Δ*xadA2* mutants showed about twofold fewer symptomatic leaves than that in plants inoculated with the WT strain at all sampling periods. On the other hand, plants inoculated with Δ*xadA3* showed increased disease severity (about 2.5-fold more symptomatic leaves) at all sampling periods compared with the WT strain (Supplementary Fig. S3). Assessment of area under disease progress curves (AUDPC) for the various strains revealed that disease severity conferred by the Δ*xadA3* mutant was significantly higher than that of the WT strain (Fig. 4B).

**Deletion of *xadA* genes cause small but highly relevant changes in gene expression profiles.**

To determine if the deletion of a given *xadA* locus would interfere with other cellular processes besides the putative primary function of TAA-mediated adhesion, we compared the gene expression profiles of the three Δ*xadA* mutants and WT (strain Temecula1) cultivated in PWG broth for 7 days by RNA-seq. The fragments per kilobase per million reads (FPKM) and transcripts per million reads (TPM) values for each gene in each biological replicate of each strain are listed in Supplementary Tables S1 and S2. TPM averages revealed that about 93% of the expressed transcripts (TPM > 0) recovered from the Δ*xadA* mutants and the WT strain (totaling 1,944 genes) were similar (Fig. 5A). As expected, transcripts corresponding to the deleted gene were absent in the respective Δ*xadA* mutant (Fig. 5B). Importantly, the TPM counts observed for *xadA1* transcripts were

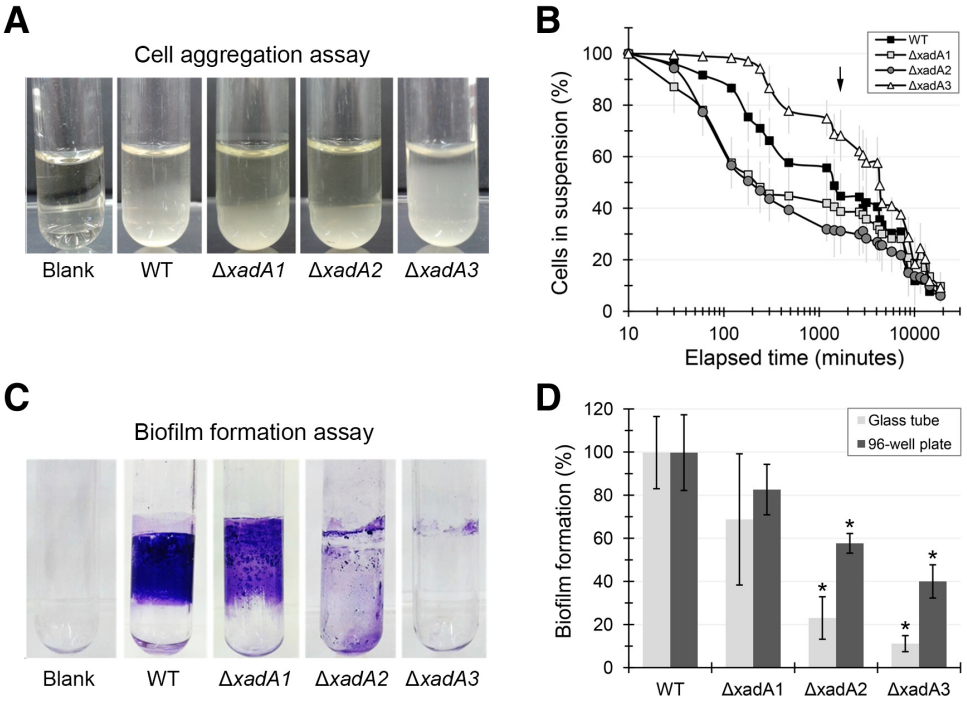


**Fig. 2.** Cell aggregation and biofilm formation by *Xylella fastidiosa* Δ*xadA* mutant strains. **A,** Cell-cell aggregation phenotype of *X. fastidiosa* wild type (WT) and mutant strains after incubation for 24 h in a periwinkle wilt medium (Davis et al. 1981) containing 0.5% glucose without bovine serum albumin (PWG) broth. **B,** Percentage of *X. fastidiosa* cells remaining in suspension in still cultures as a function of time after growth in PWG broth. The arrow indicates 24 h after the start of the assay. Shown is the mean ± standard deviation (SD) of three biological replicates with three technical triplicates each. **C,** Biofilm formed by WT and mutant strains grown in PWG broth for 14 days in glass tubes and then stained with 0.1% crystal violet. **D,** Biofilm formed by WT and mutant strains grown in PWG broth in glass tubes or 96-well plastic plates for 14 days and assessed by crystal violet staining. Shown is the mean ± SD of three biological replicates with three technical triplicates each, normalized for that of the WT strain. Values significantly ($P < 0.01$ in a homoscedastic *t* test) different from WT are noted with an asterisk.

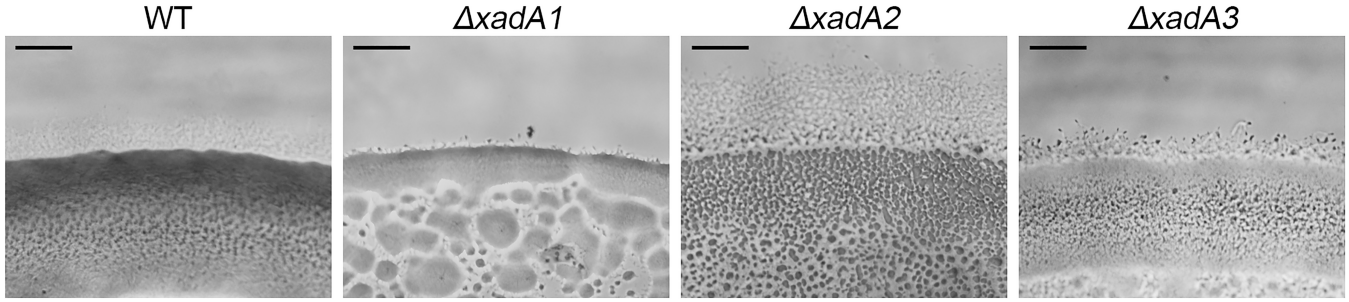


**Fig. 3.** Twitching motility of wild type (WT) and Δ*xadA* mutants. Images show colonies of WT and Δ*xadA* mutants grown on PIM6 medium. Colonies were observed after incubation for 7 days at 28°C. Scale bar = 200 μm.

13.9- and 24.7-fold higher in Δ*xadA2* and Δ*xadA3* mutants, respectively, compared with the WT strain. Similarly, the *xadA3* TPM counts were 25.6-fold higher in the Δ*xadA2* mutant than that in the WT strain. Conversely, *xadA2* and *xadA3* transcript abundance in the Δ*xadA1* mutant did not differ from that in the WT strain (Fig. 5B). It thus appears that the loss of *xadA2* or *xadA3* causes a corresponding increase in expression of the other gene encoding a TAA adhesin, which could not be observed for the loss of *xadA1*.

Only a few other genes were identified as differentially expressed ($P \leq 0.05$) in the Δ*xadA* mutants (Fig. 5C) according to a conservative analysis of the transcriptome sequences. Only three genes were upregulated in the Δ*xadA1* mutant compared with the WT, while 23 genes were upregulated and three were downregulated in the Δ*xadA2* mutant, and 27 were upregulated and four were downregulated in the Δ*xadA3* mutant compared with the WT strain (Supplementary Tables S3, S4, and S5). The lipase/esterases LesA (PD1703) and LesB (PD1702) were among the few genes that were upregulated in all three Δ*xadA* mutants relative to WT. Other upregulated transcripts in one or both Δ*xadA2* and Δ*xadA3* included those encoding ribosomal proteins, outer membrane protein W (PD1807), cell wall–associated hydrolase (PD1517), and fimbrillin FimA (PD0062). The transcript for the secreted protease PrtA (PD0956) was upregulated in both Δ*xadA1* and Δ*xadA3*.

## DISCUSSION

The three genes encoding typical TAAs, named XadA1, XadA2, and XadA3, are highly conserved among the *X. fastidiosa* genomes (Uceda-Campos et al. 2022). These proteins are membrane-associated and are located at the cell surface (Caserta et al. 2010; Feitosa-Junior et al. 2019; Ionescu et al. 2014; Nascimento et al. 2016; Smolka et al. 2003), as predicted by in-silico analyses. Both XadA1 and XadA2 had previously been shown to be involved in biofilm formation (Caserta et al. 2010; Feil et al. 2007), and XadA2 was shown to be involved in vector transmission and binding to host polysaccharides (Esteves et al. 2020). Here, we show that XadA3 strongly contributes to both cell-cell aggregation and to biofilm formation on both glass and plastic surfaces. This finding supports the previous observation that XadA3 transcript abundance was reduced in the biofilm-deficient *X. fastidiosa prtA* mutant (Gouran et al. 2016). Our results also confirm a distinct role for both XadA1 and XadA2 in biofilm formation but not in cell-cell aggregation, since their abolishment did not reduce the sedimentation of cell suspensions. Moreover, given that the adhesion of all Δ*xadA* mutants to surfaces under flow conditions was not appreciably impaired, the reduced biofilm formation observed, most apparent in Δ*xadA3*, is likely due to its deficiency in cell-cell aggregation and not in attachment of cells to the artificial surfaces tested. Further support for this assumption is provided by the demonstration of the preferential localization of XadA3 on the cell surface when in contact with other cells but not at the cell poles. Other *X. fastidiosa* proteins also exhibit localized distribution within the cell. For example, the adhesive chaperone-usher pili (type I pili) that confer strong surface attachment under flow conditions (De La Fuente et al. 2007) is located at the cell poles. It remains unclear what processes might mediate the apparent localization of XadA3 to points of contact with other cells.

Additional evidence for the role of XadA3 in cell-cell aggregation is suggested by the observation that its transcript is upregulated in Δ*xadA2*, whose cells clump faster in suspension than either Δ*xadA3* or the WT strain. Curiously, Δ*xadA1* cells also aggregated faster than WT cells, yet neither *xadA3* nor other adhesins transcripts were upregulated in this mutant. Thus, we speculate that XadA1 has a suppressive effect on cell-cell adhesion. We cannot ignore the fact that, although Δ*xadA3* exhibits both reduced cell-cell aggregation and biofilm formation under our experimental conditions, both *xadA1* and *xadA2* transcripts are upregulated in this mutant. Elevated expression of both adhesins could at least partially compensate for the absence of XadA3, but, as we have shown here, Δ*xadA3* is greatly impaired in biofilm formation. It should be noted that, although glass surfaces are routinely employed in studies of surface attachment and biofilm formation (Chen and De La Fuente 2020; De La Fuente et al. 2007; Ionescu et al. 2014; Lorite et al. 2013; Meng et al. 2005), they might not mimic the surfaces in plants and insects to which *X. fastidiosa* interacts. It remains to be explored if the various XadA proteins differ in their binding affinity to the chemically distinct surfaces in insects and plant tissues. Such differences might be expected and could

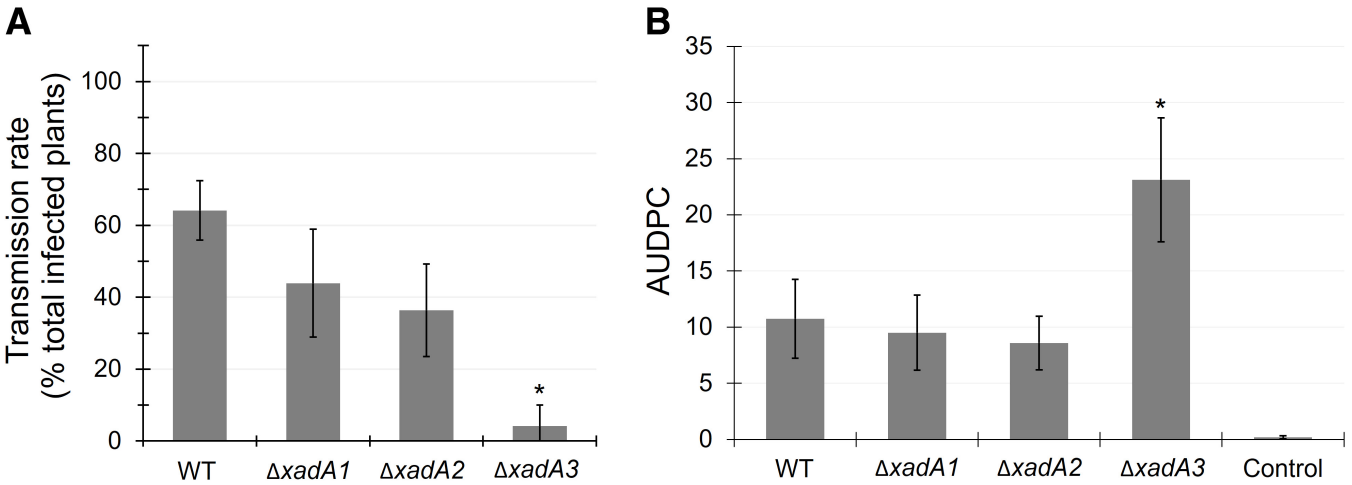


**Fig. 4.** Insect transmissibility and virulence of *Xylella fastidiosa* Δ*xadA* mutants in grapevine. **A,** Transmission efficiency by insect vectors, shown as the percentage of the 24 plants exposed to *Graphocephala atropunctata* that had fed on the various *X. fastidiosa* strains shown on the abscissa that subsequently harbored detectable cells of the pathogen. Values significantly different from wild type (WT) are noted with an asterisk ($P < 0.01$ in a homoscedastic *t* test). **B,** Virulence of WT and *xadA* mutants in grapevines. Shown is the area under the disease progress curve (AUDPC) calculated from the number of symptomatic leaves from each of 12 replicate plants for each strain that showed symptoms of Pierce's disease when assessed at various times after inoculation. The disease progress curve is shown in Supplementary Figure S3. The vertical bars indicate the standard error of the mean. Values different from WT are noted with an asterisk ($P < 0.06$ in a homoscedastic *t* test).

explain the apparent differential roles XadA proteins play on cell adhesion to glass surfaces. In support of such a conjecture, XadA2 was recently shown to have an important role in the binding to and biofilm formation of *X. fastidiosa* subsp. *pauca* on insect vector surfaces (Esteves et al. 2020). Further elucidation of a selective role of the XadAs in various disease processes would facilitate strategies focused on disruption of processes such as transmission of the pathogen to achieve disease control.

Surprisingly, the XadA deletion mutants differed in their active motility by twitching. Elimination of XadA1 had little effect on twitching motility, apparently since it, at least in part, is secreted as a component of OMVs (Caserta et al. 2010; Ionescu et al. 2014) and appears to have a little positive role in cell-cell contact. The enhanced motility of Δ*xadA2* and Δ*xadA3* suggests that these adhesins inhibit twitching, perhaps because of their primary role of facilitating cell-cell contact. It seems likely that twitching would be less successful when cells are linked together. Movement mediated by retraction of the type IV pili would need to be coordinated, in such a scenario, for linked cells to move. Δ*xadA2* and Δ*xadA3* mutants, by being more independent of each other in colonies, due to the absence of these adhesins, might thus be less-impaired in their exploration of their local environment by twitching.

The localized distribution of XadA3 on the cell surface might explain why the Δ*xadA3* mutant was not efficiently transmitted to new plants with the same efficiency as the wild-type strain. Acquisition of and retention of cells by the insect vector is an important first step in the transmission process (Killiny and Almeida 2009b). Since cells align polarly in the foregut of vectors (Almeida and Purcell 2006; Newman et al. 2004), the lack of one of the lateral adhesins important for binding of pathogen cells to each other might make them more prone to being displaced and eliminated by the rapid xylem sap flow during insect feeding (Ranieri et al. 2020). Conversely, the reduced ability to form biofilms within the plant would facilitate the spreading of the bacteria and colonization of the host, thus increasing the virulence of the pathogen (Lindow et al. 2014). Indeed, the Δ*xadA3* mutant incited significantly higher numbers of symptomatic leaves than the WT strain, suggesting that it moved more readily within the plant. The roles of TAAs in *X. fastidiosa* biology are thus complex, with apparently

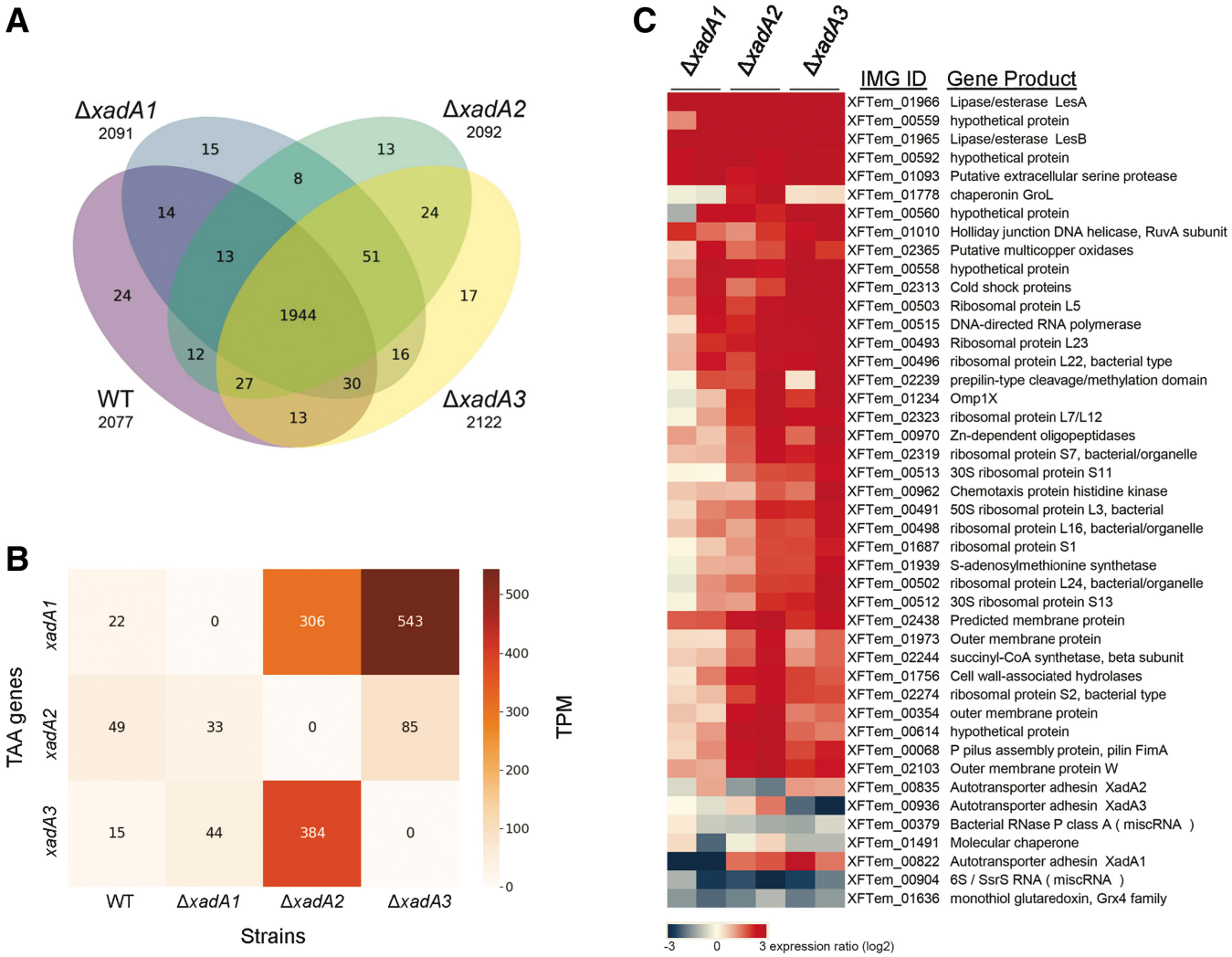


**Fig. 5.** Gene expression profiles of *xadA* mutants. Gene expression profiles of the three Δ*xadA* mutants and wild type (WT) Temecula1 strain cultivated in periwinkle wilt medium (Davis et al. 1981) containing 0.5% glucose without bovine serum albumin (PWG) broth for 7 days were assessed by RNA-seq. **A,** Venn diagram of expressed genes in the WT and Δ*xadA* mutant strains. **B,** Effect of each individual *xadA* gene deletion on expression of the *xadA* transcripts based on transcripts per million reads (TPM). **C,** Heatmap of differentially expressed genes in Δ*xadA* mutants. Expression ratios were calculated between each Δ*xadA* mutant and the WT. Genes significantly ($P < 0.05$) up- and downregulated in Δ*xadA* mutants are represented in red and blue, respectively. Genes considered not differentially expressed are colored gray.

conflicting roles in insect acquisition and retention and in plant virulence (Fig. 6). The relatively large number of adhesins in *X. fastidiosa* might enable more nuanced regulation of the adhesiveness of cells in different biological contexts. Further exploration of the expression of these adhesins and the properties of cells recovered directly from plants and insects should prove illuminating.

Analysis of the gene expression profiles of the various Δ*xadA* mutants provided insights that help explain the phenotypes associated to the loss of a particular XadA protein. Although the absence of a given XadA resulted in somewhat different effects on cell aggregation, biofilm formation, and motility, the expression of *lesA* and *lesB* was increased in all cases. Lipase/esterase LesA has been identified as a secreted *X. fastidiosa* virulence factor associated with its OMVs and linked to the symptoms of leaf scorching and chlorosis (Nascimento et al. 2016). Δ*xadA3*, having the highest differential expression of LesA of the Δ*xadA* mutants, also produced higher leaf-scorch symptoms on inoculated plants. It is possible that some of the differences in virulence observed in the Δ*xadA* mutants might be due to secondary effects of genes whose expression is linked to features of the cell envelope. Considering that other afimbrial and fimbrial adhesin mutants have been shown to be deficient in biofilm formation (Feil et al. 2007; Guilhabert and Kirkpatrick 2005; Li et al. 2007), a phenotype shared to some degree with the Δ*xadA* mutants examined here, it becomes evident that no single adhesin is sufficient for biofilm development and, instead, that several are necessary for *X. fastidiosa* to produce a robust surface-attached biofilm. This is relevant because biofilm formation is a key process in *X. fastidiosa* colonization of plant hosts and insect vectors (Chatterjee et al. 2008; Killiny and Almeida 2009b; Rapicavoli et al. 2018; Sicard et al. 2018). Understanding the importance of adhesive proteins and their individual contributions to different aspects of *X. fastidiosa* biology can guide new approaches to block vector transmission (Labroussaa et al. 2016; Killiny et al. 2012) and control disease development.

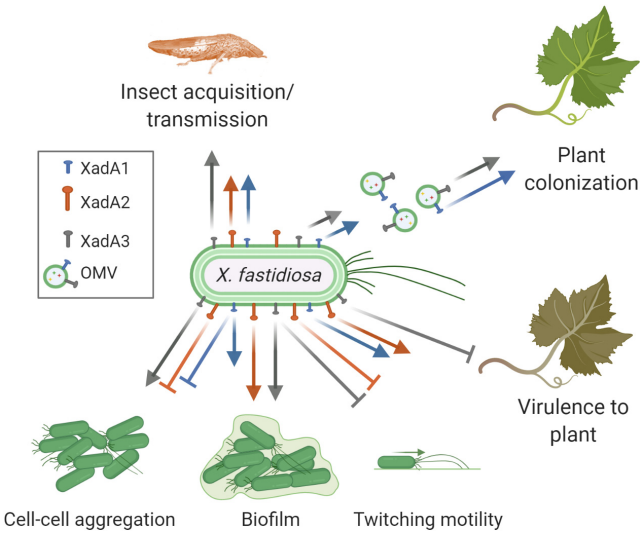


**Fig. 6.** A model for trimeric autotransporters adhesins roles in *Xylella fastidiosa*. XadA1, XadA2, and XadA3 are depicted as icons in different colors and sizes in the surface of a *X. fastidiosa* cell and in the surface of outer membrane vesicles (OMV). Short and long pili are generally located at one pole of a *X. fastidiosa* cell as represented in the scheme. Increase (arrows) or reduction (bar-headed lines) effects in the various cellular behaviors of *X. fastidiosa* both in vitro and in vivo for the distinct XadA are indicated using the same color of XadA icons. The different lengths of the arrows reflect the relative contribution of the particular adhesin to the process being depicted. Created with BioRender.

## MATERIALS AND METHODS

### Bacterial strains.

The bacterial strains and plasmids used in this work are listed in Supplementary Table S6. WT strain *X. fastidiosa* Temecula1 was used in all experiments. Δ*xadA*1 (PD0731) (Ionescu et al. 2014), Δ*xadA*2 (PD0744), and Δ*xadA*3 (PD0824) mutants were constructed by transforming the WT strain with constructs derived from pFXF*kan* (de Souza et al. 2013). To generate pFXF1 (*xadA1*::*kanR*) (Ionescu et al. 2014), pFXF2 (*xadA2*::*kanR*), and pFXF3 (*xadA3*::*kanR*), regions (900 to 1,000-bp) flanking the target locus were amplified from the Temecula1 genome using primers listed in Supplementary Table S7 and were cloned in pFXF*kan* flanking the kanamycin-resistance gene. The suicide vector constructs were transformed in WT utilizing its natural competence (Kung and Almeida 2011). Transformed cells were plated on PW (periwinkle wilt medium) (Davis et al. 1981) with 1% Gelrite (Merck, Darmstadt, Germany) supplemented with kanamycin. After 2 to 3 weeks of incubation at 28°C, kanamycin-resistant colonies were verified for the deletion of *xadA1*, *xadA2*, or *xadA3*, using the primers listed in Supplementary Table S7. Gene deletion was confirmed by sequencing the PCR product amplified from genomic DNA purified from the selected mutant strains. Loss of the respective XadA protein in each deletion mutant was further confirmed with anti-XadA1, anti-XadA2, and anti-XadA3 polyclonal antibodies (Supplementary Fig. S4).

### *X. fastidiosa* culture conditions.

*X. fastidiosa* strains were routinely cultured in PWG medium (Davis et al. 1981) for 7 to 21 days at 28°C in a rotary shaker (100 to 170 rpm) or in PW with 1% Gelrite (Merck, Darmstadt, Germany) for 7 to 21 days at 28°C. Strains were cultured on agar plates of PWG or PIM6 medium (Ionescu et al. 2014) for 7 days at 28°C for observation of twitching motility on the peripheries of the colonies, using a dissecting microscope.

### Biofilm formation.

Biofilm formation was assessed in both 96-well plates and glass tubes as previously described (Fogaca et al. 2010; Zaini et al. 2009). Seven-day-old bacterial cultures with optical densities at 600 nm ($OD_{600nm}$) adjusted to 0.05 and 2 ml of bacterial suspensions were transferred to glass tubes and were incubated for 14 days at 28°C in a rotary shaker (170 rpm). Planktonic cells and medium were discarded, and the remaining biofilm was carefully rinsed twice with distilled water and was stained for 20 min with 2.5 ml of 0.1% aqueous crystal violet solution. Tubes were rinsed twice; biofilm was dispersed with 2 ml of 1% sodium dodecyl sulfate (SDS) and the absorbance at 595 nm was determined. For assays in 96-well plates, 150 µl of bacterial culture ($OD_{600nm} = 0.05$) was transferred to wells and the plate was incubated for 14 days at 28°C in a rotary shaker (170 rpm). After staining with aqueous crystal violet as above, absorbance at 595 nm was determined with a SpectraMax Paradigm (Molecular Devices, San Jose, CA, U.S.A.).

### Cell-cell aggregation.

Cell-cell aggregation was accessed in agglutination assays as described before (Guilhabert and Kirkpatrick 2005). Briefly, bacterial suspensions in PWG were adjusted to $OD_{600nm} = 2.0$, 2 ml was transferred to 15-ml tubes, and was maintained without shaking at room temperature. After various incubation times, 1ml was withdrawn from the upper half of the tube and the $OD_{600nm}$ was evaluated. Statistical significance between samples was determined at $P < 0.01$ in a homoscedastic *t* test.

**Cell-surface attachment in microfluidic chambers.**

Polydimethylsiloxane-borosilicate glass chambers containing observation channels of 50 × 100 μm were built, as described by Meng et al. (2005), using a spin-coated photoresist wafer mold purchased from the McGill University Advanced Nano Design Applications Facility. Cell-surface attachment assays were performed as previously described (De La Fuente et al. 2007) with modifications. The chamber was filled with a flow of PWG prior to injection of 200 μl of a cell suspension ($10^7$ cells per milliliter). Unbound cells were removed by slowly passing medium (3 mm/s) through the chamber, resulting in approximately 50 cells remaining in an observation field. After 15 min under the initial flow condition, the remaining bound cells were photographed and were tracked individually during subsequent 5-min steps in which flow speed was increased incrementally from 3 to 700 mm/s, which are biologically relevant speeds yet potentially below maximum speeds estimated within insects (Ranieri et al. 2020). At the end of each flow interval, cells were photographed and counted. In assays to verify the effect of anti-XadA3 on attachment, cells were incubated for 30 min with anti-Xad3 serum (1:100), pre-immune serum (1:100), or phosphate buffered saline, before injection into the chamber. Statistical significance between samples and control was determined at $P < 0.02$ in a homoscedastic *t* test.

**Immunodetection of XadA proteins.**

For immunoblotting, bacterial cell pellets were lysed by sonication in cold lysis buffer (50 mM Tris [pH 8.0], 10% glycerol containing Roche complete protease inhibitor [Merck, Darmstadt, Germany]), 10 μg of total protein were separated by 10% SDS-polyacrylamide gel electrophoresis (Laemmli 1970) and were electro-blotted onto nitrocellulose membrane (Kurien and Scofield 2003). Membranes were probed for 16 h at 8°C with anti-XadA1 (1:10,000), anti-XadA2 (1:400), and anti-XadA3 (1:2,000) antisera diluted in TBST (200 mM Tris-HCl [pH 7.4], 150 mM NaCl, 0.1% Tween 20) with 5% nonfat powdered milk. Membranes were washed six times for 5 min each with TBST at 22°C and were incubated with IRDye800CW anti-rabbit immunoglobulin G secondary antibody (Li-Cor, Lincoln, NE, U.S.A.) at 1:15,000 for 1 h at 22°C. After several washes with TBST, images were captured in an Odyssey infrared imaging system (Li-Cor). Polyclonal antibodies anti-XadA1 and anti-XadA2 were obtained in rabbits (Caserta et al. 2010). Anti-XadA3 was obtained in rabbits by injection of purified recombinant protein corresponding to a 451-aa fragment of the N-terminal portion of XadA3. The recombinant protein (about 46 kDa) with a His-tag on its C terminal was obtained by cloning the N-terminal sequence of *xadA3* (XF1981) encoded in the *X. fastidiosa* 9a5c genome (Simpson et al. 2000) in Novagen pET28a and expression in *Escherichia coli* BL21-Gold (DE3) (Agilent Technologies, Santa Clara, CA. U.S.A.).

**Plant inoculation and insect transmission.**

*Vitis vinifera* Cabernet Sauvignon seedlings were grown in a greenhouse to a height of 50 cm and were mechanically inoculated with the WT and mutant strains of *X. fastidiosa*, using delicate perforations at the base of a petiole after adding a drop (5 μl) of bacterial cell suspension ($10^8$ cells per milliliter) as described (Baccari and Lindow 2011). The number of symptomatic leaves (exhibiting loss of chlorophyll and death of the leaf margins) was counted weekly, starting at 7 weeks after inoculation (Ionescu et al. 2013). AUDPC was calculated (Simko and Piepho 2011) from the number of symptomatic leaves of each plant. For insect transmission assays, 30 to 40 insects (Hemiptera, Cicadellidae, *Graphocephala atropunctata*, blue-green sharpshooter) were fed on an artificial diet device with a given bacterial strain for 3 days, as before (Baccari et al. 2014; Labroussaa et al. 2016; Killiny and Almeida 2009a). The insects were then transferred to an uninfected plant for an inoculation access period of 7 days. After this inoculation period, these plants were kept in a greenhouse for at least 8 weeks. Presence of *X. fastidiosa* in grapevines was determined by culturing of petiole macerates in PW plates and diagnostic PCR. Twenty-four plants were exposed to vectors for each *X. fastidiosa* strain in each of two biological replicates. Statistical significance between samples was determined at $P < 0.05$ in a homoscedastic *t* test.

**Transcriptome analysis.**

Total RNA was isolated from 50 ml of *X. fastidiosa* cultures (WT, Δ*xadA1*, Δ*xadA2*, and Δ*xadA3*) using Trizol reagent and Pure Link RNA mini kit (Thermo Fisher Scientific, Waltham, MA, U.S.A.). RNA samples (15 μg) were further purified with Illustra RNASpin Mini RNA isolation Kit (GE Healthcare Life Sciences, Marlborough, MA, U.S.A.) for removal of residual genomic DNA. Ribosomal RNA (rRNA) was removed from RNA samples (5 μg) with Ribo-Zero rRNA removal kit (Illumina, San Diego, CA, U.S.A.), and RNA was immediately used for preparation of RNA-seq libraries, using the Illumina TruSeq RNA sample preparation kit v2 (Illumina). The libraries were paired-end sequenced with a MiSeq-Illumina platform using the MiSeq Reagent kit v2 (500-cycle format). When required, the concentration of RNA samples was evaluated as the absorbance at 260, 280, and 230 nm on a NanoDrop ND-2000 Spectrophotometer (Thermo Fisher Scientific) or with Quant-iT RiboGreen RNA assay kit (Thermo Fisher Scientific). RNA integrity (RIN > 7.5) and rRNA depletion efficiency were verified by electrophoresis on a 2100 Bioanalyzer (Agilent Technologies). FASTQ files of Illumina paired-end reads (2 × 250 bp) were processed on CLC Genomics Workbench version 6.5 (Qiagen, Hilden, Germany) for quality-filtering (quality score ≥ 30) and adapters removal. Contaminant rRNA sequences in some of the complementary DNA libraries were removed using riboPicker (Schmieder et al. 2011). Filtered reads were mapped on the Temecula1 genome (Van Sluys et al. 2003), which was reannotated using the Integrated Microbial Genomes and Microbiomes (IMG/M) data management system (Chen et al. 2019) and FPKM (Mortazavi et al. 2008) values for each transcript were exported from the CLC Genomics Workbench. TPM values were obtained through the conversion from FPKM values using the equation $TPM_i = 10^6 \times (FPKM_i \div \Sigma FPKM_j)$, as described by Zhao et al. (2020). Genes differentially expressed between a mutant strain (Δ*xadA1*, Δ*xadA2*, Δ*xadA3*) and the WT were identified using the DESeq2 R package (Love et al. 2014), using RNA-seq data from two biological replicates. Genes presenting $\log_2$ fold change with an adjusted *P* value ≤ 0.05 were assigned as differentially expressed. Heatmap and Venn diagrams were generated, respectively, with seaborn and Venn Python libraries using plotting library matplotlib (Python-Core-Team 2015).

**Analyses of protein sequences.**

Protein domain analysis was performed using Pfam release 33.1 (El-Gebali et al. 2019). Subcellular localization of proteins was predicted with SignalP v5.0 (Armenteros et al. 2019), SecretomeP v2.0 (Bendtsen et al. 2005), and PSORTb v3.0 (Yu et al. 2010) servers. Protein structure three-dimensional models were obtained with Phyre2 Protein Homology/analogY Recognition Engine v2.0 (Kelley et al. 2015). YadA-anchor domains of selected bacterial species were used to construct a maximum likelihood–based tree, using IQ-Tree v1.6 software (Nguyen et al. 2015).

**Availability of sequence data.**

Transcriptome sequencing (RNA-seq) data reported in this work have been deposited in the National Center for Bio-

technology Information Short Read Archive database under BioProject accession number PRJNA667756. Reannotation of *X. fastidiosa* Temecula1 genome (Van Sluys et al. 2003) is available at IMG/M (Chen et al. 2019) under taxon ID 2514752010.

## ACKNOWLEDGMENTS

We thank A. A. de Souza (Centro de Citricultura Sylvio Moreira, Instituto Agronômico de Campinas) for providing anti-XadA1 and anti-XadA2 polyclonal sera.

## LITERATURE CITED

Almeida, R. P. P., and Purcell, A. H. 2006. Patterns of *Xylella fastidiosa* colonization on the precibarium of sharpshooter vectors relative to transmission to plants. Ann. Entomol. Soc. Am. 99:884-890.

Armenteros, J. J. A., Tsirigos, K. D., Sonderby, C. K., Petersen, T. N., Winther, O., Brunak, S., von Heijne, G., and Nielsen, H. 2019. SignalP 5.0 improves signal peptide predictions using deep neural networks. Nat. Biotechnol. 37:420-423.

Baccari, C., Killiny, N., Ionescu, M., Almeida, R. P. P., and Lindow, S. E. 2014. Diffusible Signal Factor-repressed extracellular traits enable attachment of *Xylella fastidiosa* to insect vectors and transmission. Phytopathology 104:27-33.

Baccari, C., and Lindow, S. E. 2011. Assessment of the process of movement of *Xylella fastidiosa* within susceptible and resistant grape cultivars. Phytopathology 101:77-84.

Bendtsen, J. D., Kiemer, L., Fausboll, A., and Brunak, S. 2005. Non-classical protein secretion in bacteria. BMC Microbiol. 5:ARTN 58.

Caserta, R., Takita, M. A., Targon, M. L., Rosselli-Murai, L. K., de Souza, A. P., Peroni, L., Stach-Machado, D. R., Andrade, A., Labate, C. A., Kitajima, E. W., Machado, M. A., and de Souza, A. A. 2010. Expression of *Xylella fastidiosa* fimbrial and afimbrial proteins during biofilm formation. Appl. Environ. Microbiol. 76:4250-4259.

Chatterjee, S., Almeida, R. P. P., and Lindow, S. 2008. Living in two worlds: The plant and insect lifestyles of *Xylella fastidiosa*. Annu. Rev. Phytopathol. 46:243-271.

Chen, H., and De La Fuente, L. 2020. Calcium transcriptionally regulates movement, recombination and other functions of *Xylella fastidiosa* under constant flow inside microfluidic chambers. Microb. Biotechnol. 13: 548-561.

Chen, I. A., Chu, K., Palaniappan, K., Pillay, M., Ratner, A., Huang, J., Huntemann, M., Varghese, N., White, J. R., Seshadri, R., Smirnova, T., Kirton, E., Jungbluth, S. P., Woyke, T., Eloe-Fadrosh, E. A., Ivanova, N. N., and Kyrpides, N. C. 2019. IMG/M v.5.0: An integrated data management and comparative analysis system for microbial genomes and microbiomes. Nucleic Acids Res. 47:D666-D677.

Danhorn, T., and Fuqua, C. 2007. Biofilm formation by plant-associated bacteria. Annu. Rev. Microbiol. 61:401-422.

Davis, M. J., French, W. J., and Schaad, N. W. 1981. Axenic culture of the bacteria associated with phony disease of peach and plum leaf scald. Curr. Microbiol. 6:309-314.

De La Fuente, L., Montanes, E., Meng, Y. Z., Li, Y. X., Burr, T. J., Hoch, H. C., and Wu, M. M. 2007. Assessing adhesion forces of type I and type IV pili of *Xylella fastidiosa* bacteria by use of a microfluidic flow chamber. Appl. Environ. Microbiol. 73:2690-2696.

de Souza, A. A., Ionescu, M., Baccari, C., da Silva, A. M., and Lindow, S. E. 2013. Phenotype overlap in *Xylella fastidiosa* is controlled by the cyclic di-GMP phosphodiesterase Eal in response to antibiotic exposure and diffusible signal factor-mediated cell-cell signaling. Appl. Environ. Microbiol. 79:3444-3454.

de Souza, A. A., Takita, M. A., Coletta, H. D., Caldana, C., Goldman, G. H., Yanai, G. M., Muto, N. H., de Oliveira, R. C., Nunes, L. R., and Machado, M. A. 2003. Analysis of gene expression in two growth states of *Xylella fastidiosa* and its relationship with pathogenicity. Mol. Plant-Microbe Interact. 16:867-875.

de Souza, A. A., Takita, M. A., Pereira, E. O., Coletta, H. D., and Machado, M. A. 2005. Expression of pathogenicity-related genes of *Xylella fastidiosa* in vitro and in planta. Curr. Microbiol. 50:223-228.

El-Gebali, S., Mistry, J., Bateman, A., Eddy, S. R., Luciani, A., Potter, S. C., Qureshi, M., Richardson, L. J., Salazar, G. A., Smart, A., Sonnhammer, E. L. L., Hirsh, L., Paladin, L., Piovesan, D., Tosatto, S. C. E., and Finn, R. D. 2019. The Pfam protein families database in 2019. Nucleic Acids Res. 47:D427-D432.

Esteves, M. B., Lopes Nalin, J., Kudlawiec, K., Caserta Salviatto, R., de Melo Sales, T., Sicard, A., Piacentini Paes de Almeida, R., Alves de Souza, A., and Roberto Spotti Lopes, J. 2020. XadA2 adhesin decreases biofilm formation and transmission of *Xylella fastidiosa* subsp. *pauca*. Insects 11:473.

Fan, E., Chauhan, N., Udatha, D. B. R. K. G., Leo, J. C., and Linke, D. 2016. Type V secretion systems in bacteria. Microbiol. Spectr. 4.

Feil, H., Feil, W. S., and Lindow, S. E. 2007. Contribution of fimbrial and afimbrial adhesins of *Xylella fastidiosa* to attachment to surfaces and virulence to grape. Phytopathology 97:318-324.

Feitosa-Junior, O. R., Stefanello, E., Zaini, P. A., Nascimento, R., Pierry, P. M., Dandekar, A. M., Lindow, S. E., and da Silva, A. M. 2019. Proteomic and metabolomic analyses of *Xylella fastidiosa* OMV-enriched fractions reveal association with virulence factors and signaling molecules of the DSF family. Phytopathology 109:1344-1353.

Fogaca, A. C., Zaini, P. A., Wulff, N. A., da Silva, P. I. P., Fazio, M. A., Miranda, A., Daffre, S., and da Silva, A. M. 2010. Effects of the antimicrobial peptide gomesin on the global gene expression profile, virulence and biofilm formation of *Xylella fastidiosa*. FEMS Microbiol. Lett. 306:152-159.

Python-Core-Team. 2015. Python: A dynamic, open source programming language. Python Software Foundation, Beaverton, OR, U.S.A.

Gouran, H., Gillespie, H., Nascimento, R., Chakraborty, S., Zaini, P. A., Jacobson, A., Phinney, B. S., Dolan, D., Durbin-Johnson, B. P., Antonova, E. S., Lindow, S. E., Mellema, M. S., Goulart, L. R., and Dandekar, A. M. 2016. The secreted protease PrtA controls cell growth, biofilm formation and pathogenicity in *Xylella fastidiosa*. Sci. Rep. 6:13.

Guilhabert, M. R., and Kirkpatrick, B. C. 2005. Identification of *Xylella fastidiosa* antivirulence genes: Hemagglutinin adhesins contribute to *X. fastidiosa* biofilm maturation and colonization and attenuate virulence. Mol. Plant-Microbe Interact. 18:856-868.

Hartmann, M. D., Grin, I., Dunin-Horkawicz, S., Deiss, S., Linke, D., Lupas, A. N., and Hernandez Alvarez, B. 2012. Complete fiber structures of complex trimeric autotransporter adhesins conserved in enterobacteria. Proc. Nat. Acad. Sci. U.S.A. 109:20907.

Ionescu, M., Baccari, C., Da Silva, A. M., Garcia, A., Yokota, K., and Lindow, S. E. 2013. Diffusible Signal Factor (DSF) synthase RpfF of *Xylella fastidiosa* is a multifunction protein also required for response to DSF. J. Bacteriol. 195:5273-5284.

Ionescu, M., Zaini, P. A., Baccari, C., Tran, S., da Silva, A. M., and Lindow, S. E. 2014. *Xylella fastidiosa* outer membrane vesicles modulate plant colonization by blocking attachment to surfaces. Proc. Nat. Acad. Sci. U.S.A. 111:E3910-E3918.

Kelley, L. A., Mezulis, S., Yates, C. M., Wass, M. N., and Sternberg, M. J. E. 2015. The Phyre2 web portal for protein modeling, prediction and analysis. Nat. Protoc. 10:845-858.

Killiny, N., and Almeida, R. P. P. 2009a. Host structural carbohydrate induces vector transmission of a bacterial plant pathogen. Proc. Nat. Acad. Sci. U.S.A. 106:22416-22420.

Killiny, N., and Almeida, R. P. P. 2009b. *Xylella fastidiosa* afimbrial adhesins mediate cell transmission to plants by leafhopper vectors. Appl. Environ. Microbiol. 75:521-528.

Killiny, N., and Almeida, R. P. P. 2014. Factors affecting the initial adhesion and retention of the plant pathogen *Xylella fastidiosa* in the foregut of an insect vector. Appl. Environ. Microbiol. 80:420-426.

Killiny, N., Martinez, R. H., Dumenyo, C. K., Cooksey, D. A., and Almeida, R. P. P. 2013. The exopolysaccharide of *Xylella fastidiosa* is essential for biofilm formation, plant virulence, and vector transmission. Mol. Plant-Microbe Interact. 26:1044-1053.

Killiny, N., Rashed, A., and Almeida, R. P. P. 2012. Disrupting the transmission of a vector-borne plant pathogen. Appl. Environ. Microbiol. 78: 638-643.

Kung, S. H., and Almeida, R. P. P. 2011. Natural competence and recombination in the plant pathogen *Xylella fastidiosa*. Appl. Environ. Microbiol. 77:5278-5284.

Kurien, B. T., and Scofield, R. H. 2003. Protein blotting: A review. J. Immunol. Methods 274:1-15.

Labroussaa, F., Zeilinger, A. R., and Almeida, R. P. P. 2016. Blocking the transmission of a noncirculative vector-borne plant pathogenic bacterium. Mol. Plant-Microbe Interact. 29:535-544.

Laemmli, U. K. 1970. Cleavage of structural proteins during the assembly of the head of bacteriophage T4. Nature 227:680-685.

Li, Y. X., Hao, G. X., Galvani, C. D., Meng, Y. Z., De la Fuente, L., Hoch, H. C., and Burr, T. J. 2007. Type I and type IV pili of *Xylella fastidiosa* affect twitching motility, biofilm formation and cell-cell aggregation. Microbiology-Sgm 153:719-726.

Lindow, S., Newman, K., Chatterjee, S., Baccari, C., Lavarone, A. T., and Ionescu, M. 2014. Production of *Xylella fastidiosa* Diffusible Signal Factor in transgenic grape causes pathogen confusion and reduction in severity of Pierce's Disease. Mol. Plant-Microbe Interact. 27:244-254.

Lorite, G. S., Janissen, R., Clerici, J. H., Rodrigues, C. M., Tomaz, J. P., Mizaikoff, B., Kranz, C., de Souza, A. A., and Cotta, M. A. 2013. Surface physicochemical properties at the micro and nano length scales: Role on bacterial adhesion and *Xylella fastidiosa* biofilm development. PLoS One 8:e75247.

Love, M. I., Huber, W., and Anders, S. 2014. Moderated estimation of fold change and dispersion for RNA-seq data with DESeq2. Genome Biol. 15:550.

Matsumoto, A., Huston, S. L., Killiny, N., and Igo, M. M. 2012. XatA, an AT-1 autotransporter important for the virulence of *Xylella fastidiosa* Temecula1. Microbiologyopen 1:33-45.

Meng, Y. Z., Li, Y. X., Galvani, C. D., Hao, G. X., Turner, J. N., Burr, T. J., and Hoch, H. C. 2005. Upstream migration of *Xylella fastidiosa* via pilus-driven twitching motility. J. Bacteriol. 187:5560-5567.

Meuskens, I., Saragliadis, A., Leo, J. C., and Linke, D. 2019. Type V secretion systems: An overview of passenger domain functions. Front. Microbiol. 10:1163.

Mhedbi-Hajri, N., Jacques, M. A., and Koebnik, R. 2011. Adhesion mechanisms of plant-pathogenic xanthomonadaceae. Pages 71-89 in: Bacterial Adhesion: Chemistry, Biology and Physics, Vol 715. D. Linke and A. Goldman, eds. Springer, Dordrecht, The Netherlands.

Mortazavi, A., Williams, B. A., McCue, K., Schaeffer, L., and Wold, B. 2008. Mapping and quantifying mammalian transcriptomes by RNA-Seq. Nat. Methods 5:621-628.

Mühlenkamp, M., Oberhettinger, P., Leo, J. C., Linke, D., and Schütz, M. S. 2015. *Yersinia* adhesin A (YadA) – Beauty & beast. Int. J. Med. Microbiol. 305:252-258.

Nascimento, R., Gouran, H., Chakraborty, S., Gillespie, H. W., Almeida-Souza, H. O., Tu, A., Rao, B. J., Feldstein, P. A., Bruening, G., Goulart, L. R., and Dandekar, A. M. 2016. The type II secreted lipase/esterase LesA is a key virulence factor required for *Xylella fastidiosa* pathogenesis in grapevines. Sci. Rep. 6:16.

Newman, K. L., Almeida, R. P. P., Purcell, A. H., and Lindow, S. E. 2004. Cell-cell signaling controls *Xylella fastidiosa* interactions with both insects and plants. Proc. Nat. Acad. Sci. U.S.A. 101:1737-1742.

Nguyen, L.-T., Schmidt, H. A., von Haeseler, A., and Minh, B. Q. 2015. IQ-TREE: A fast and effective stochastic algorithm for estimating Maximum-Likelihood phylogenies. Mol. Biol. Evol. 32:268-274.

Ranieri, E., Zitti, G., Riolo, P., Isidoro, N., Ruschioni, S., Brocchini, M., and Almeida, R. P. P. 2020. Fluid dynamics in the functional foregut of xylem-sap feeding insects: A comparative study of two *Xylella fastidiosa* vectors. J. Insect Physiol. 120:103995.

Rapicavoli, J., Ingel, B., Blanco-Ulate, B., Cantu, D., and Roper, C. 2018. *Xylella fastidiosa*: An examination of a re-emerging plant pathogen. Mol. Plant Pathol. 19:786-800.

Roper, C., Castro, C., and Ingel, B. 2019. *Xylella fastidiosa*: Bacterial parasitism with hallmarks of commensalism. Curr. Opin. Plant Biol. 50: 140-147.

Roper, M. C., Greve, L. C., Warren, J. G., Labavitch, J. M., and Kirkpatrick, B. C. 2007. *Xylella fastidiosa* requires polygalacturonase for colonization and pathogenicity in *Vitis vinifera* grapevines. Mol. Plant-Microbe Interact. 20:411-419.

Schmieder, R., Lim, Y. W., and Edwards, R. 2011. Identification and removal of ribosomal RNA sequences from metatranscriptomes. Bioinformatics 28:433-435.

Sicard, A., Zeilinger, A. R., Vanhove, M., Schartel, T. E., Beal, D. J., Daugherty, M. P., and Almeida, R. P. P. 2018. *Xylella fastidiosa*: Insights into an Emerging Plant Pathogen. Annu. Rev. Phytopathol. 56:181-202.

Simko, I., and Piepho, H.-P. 2011. The area under the disease progress stairs: Calculation, advantage, and application. Phytopathology 102:381-389.

Simpson, A. J. G., Reinach, F. C., Arruda, P., Abreu, F. A., Acencio, M., Alvarenga, R., Alves, L. M. C., Araya, J. E., Baia, G. S., Baptista, C. S., Barros, M. H., Bonaccorsi, E. D., Bordin, S., Bove, J. M., Briones, M. R. S., Bueno, M. R. P., Camargo, A. A., Camargo, L. E. A., Carraro, D. M., Carrer, H., Colauto, N. B., Colombo, C., Costa, F. F., Costa, M. C. R., Costa-Neto, C. M., Coutinho, L. L., Cristofani, M., Dias-Neto, E., Docena, C., El-Dorry, H., Facincani, A. P., Ferreira, A. J. S., Ferreira, V. C. A., Ferro, J. A., Fraga, J. S., Franca, S. C., Franco, M. C., Frohme, M., Furlan, L. R., Garnier, M., Goldman, G. H., Goldman, M. H. S., Gomes, S. L., Gruber, A., Ho, P. L., Hoheisel, J. D., Junqueira, M. L., Kemper, E. L., Kitajima, J. P., Krieger, J. E., Kuramae, E. E., Laigret, F., Lambais, M. R., Leite, L. C. C., Lemos, E. G. M., Lemos, M. V. F., Lopes, S. A., Lopes, C. R., Machado, J. A., Machado, M. A., Madeira, A., Madeira, H. M. F., Marino, C. L., Marques, M. V., Martins, E. A. L., Martins, E. M. F., Matsukuma, A. Y., Menck, C. F. M., Miracca, E. C., Miyaki, C. Y., Monteiro-Vitorello, C. B., Moon, D. H., Nagai, M. A., Nascimento, A., Netto, L. E. S., Nhani, A., Nobrega, F. G., Nunes, L. R., Oliveira, M. A., de Oliveira, M. C., de Oliveira, R. C., Palmieri, D. A., Paris, A., Peixoto, B. R., Pereira, G. A. G., Pereira, H. A., Pesquero, J. B., Quaggio, R. B., Roberto, P. G., Rodrigues, V., Rosa, A. J. D., de Rosa, V. E., de Sa, R. G., Santelli, R. V., Sawasaki, H. E., da Silva, A. C. R., da Silva, A. M., da Silva, F. R., Silva, W. A., da Silveira, J. F., Silvestri, M. L. Z., Siqueira, W. J., de Souza, A. A., de Souza, A. P., Terenzi, M. F., Truffi, D., Tsai, S. M., Tsuhako, M. H., Vallada, H., Van Sluys, M. A., Verjovski-Almeida, S., Vettore, A. L., Zago, M. A., Zatz, M., Meidanis, J., and Setubal, J. C. 2000. The genome sequence of the plant pathogen *Xylella fastidiosa*. Nature 406:151-157.

Smolka, M. B., Martins, D., Winck, F. V., Santoro, C. E., Castellari, R. R., Ferrari, F., Brum, I. J., Galembeck, E., Coletta, H. D., Machado, M. A., Marangoni, S., and Novello, J. C. 2003. Proteome analysis of the plant pathogen *Xylella fastidiosa* reveals major cellular and extracellular proteins and a peculiar codon bias distribution. Proteomics 3:224-237.

Uceda-Campos, G., Feitosa-Junior, O. R., Santiago, C. R. N., Pierry, P. M., Zaini, P. A., de Santana, W. O., Martins-Junior, J., Barbosa, D., Digiampietri, L. A., Setubal, J. C., and da Silva, A. M. 2022. Comparative genomics of *Xylella fastidiosa* explores candidate host-specificity determinants and expands the known repertoire of mobile genetic elements and immunity systems. Microorganisms 10:914.

Van Sluys, M. A., de Oliveira, M. C., Monteiro-Vitorello, C. B., Miyaki, C. Y., Furlan, L. R., Camargo, L. E. A., da Silva, A. C. R., Moon, D. H., Takita, M. A., Lemos, E. G. M., Machado, M. A., Ferro, M. I. T., da Silva, F. R., Goldman, M. H. S., Goldman, G. H., Lemos, M. V. F., El-Dorry, H., Tsai, S. M., Carrer, H., Carraro, D. M., de Oliveira, R. C., Nunes, L. R., Siqueira, W. J., Coutinho, L. L., Kimura, E. T., Ferro, E. S., Harakava, R., Kuramae, E. E., Marino, C. L., Giglioti, E., Abreu, I. L., Alves, L. M. C., do Amaral, A. M., Baia, G. S., Blanco, S. R., Brito, M. S., Cannavan, F. S., Celestino, A. V., da Cunha, A. F., Fenille, R. C., Ferro, J. A., Formighieri, E. F., Kishi, L. T., Leoni, S. G., Oliveira, A. R., Rosa, V. E., Sassaki, F. T., Sena, J. A. D., de Souza, A. A., Truffi, D., Tsukumo, F., Yanai, G. M., Zaros, L. G., Civerolo, E. L., Simpson, A. J. G., Almeida, N. F., Setubal, J. C., and Kitajima, J. P. 2003. Comparative analyses of the complete genome sequences of Pierce's disease and citrus variegated chlorosis strains of *Xylella fastidiosa*. J. Bacteriol. 185:1018-1026.

Voegel, T. M., Warren, J. G., Matsumoto, A., Igo, M. M., and Kirkpatrick, B. C. 2010. Localization and characterization of *Xylella fastidiosa* haemagglutinin adhesins. Microbiology-Sgm 156:2172-2179.

Yu, N. Y., Wagner, J. R., Laird, M. R., Melli, G., Rey, S., Lo, R., Dao, P., Sahinalp, S. C., Ester, M., Foster, L. J., and Brinkman, F. S. L. 2010. PSORTb 3.0: Improved protein subcellular localization prediction with refined localization subcategories and predictive capabilities for all prokaryotes. Bioinformatics 26:1608-1615.

Zaini, P. A., Burdman, S., Igo, M. M., Parker, J. K., and De La Fuente, L. 2016. Fimbrial and afimbrial adhesins involved in bacterial attachment to surfaces. Pages 73-106 in: Virulence Mechanisms of Plant-Pathogenic Bacteria. N. Wang, J. B. Jones, G. W. Sundin, F. F. White, S. A. Hogenhout, C. Roper, L. De La Fuente and J. H. Ham, eds. The American Phytopathological Society, St. Paul, MN, USA.

Zaini, P. A., De La Fuente, L., Hoch, H. C., and Burr, T. J. 2009. Grapevine xylem sap enhances biofilm development by *Xylella fastidiosa*. FEMS Microbiol. Lett. 295:129-134.

Zhao, S., Ye, Z., and Stanton, R. 2020. Misuse of RPKM or TPM normalization when comparing across samples and sequencing protocols. RNA 26:903-909.